Electronic Supplementary Information

13.76% Efficiency nonfullerene solar cells enabled by selenophene integrating dithieno[3,2-*b*:2',3'-*d*]pyrrole asymmetric acceptors

Jinru Cao,[a,†] Shenya Qu,[b,†] Jiangsheng Yu,[b] Zhuohan Zhang,[a] Renyong Geng,[a] Linqiang Yang,[a] Hongtao Wang,[b] Fuqiang Du,[a] Weihua Tang,*[a]

Table of contents

S1. Experimental Section

S1.1 Materials

All chemicals and solvents were purchased from J&K, energy chemical or Sigma-Aldrich and used without further purification unless otherwise noted. Diethyl 2-bromo-5-(4-octyl-4H-dithieno[3,2-b:2',3'-d]pyrrol-2-yl)terephthalate **(1)** was synthesized according to the procedure reported in literatures. [1] The synthetic route of DTPPSe-based FRAs was shown in **Scheme S1**. The detailed synthetic procedures for DTPPSe-based FRAs are listed as below.

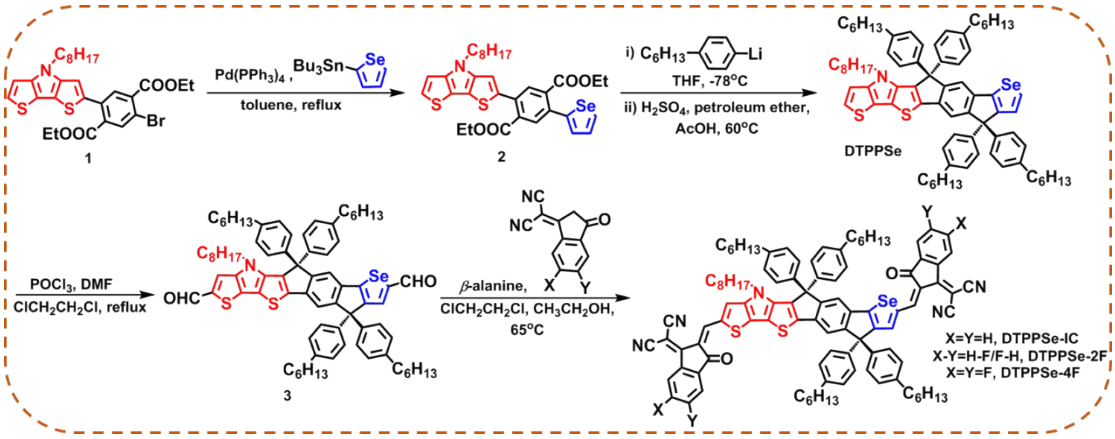

Scheme S1. Synthetic routes of DTPPSe-based FRAs.

Synthesis of ***Compound 2***.

To a solution of compound **1** (850 mg, 1.44 mmol) and tributyl- (selenophen-2-yl)stannane (907 mg, 2.16 mmol) in toluene (25 mL) was added $Pd(PPh_3)_4$ (150 mg, 0.13 mmol) under nitrogen atmosphere. The mixture was deoxygenated with nitrogen for 30 min and then refluxed for 24 h. After cooling to room temperature, the resulting mixture was poured into water (200 mL) and extracted with ethyl acetate (3×100 mL). The combined organic layers were dried over anhydrous $MgSO_4$ and filtered. The filtrate was concentrated under vacuum and purified by column chromatography on silica gel with petroleum ether/ethyl acetate (12:1) as an eluent to give a yellow liquid (550 mg, 60%) .^{1}H NMR (500 MHz, $CDCl_3$, δ): 8.08 (d, J = 5.4 Hz, 1H), 7.90 (s, 1H), 7.77 (s, 1H), 7.32 (m, J = 5.4 Hz, 1H), 7.25 (d, J = 3.2 Hz, 1H), 7.17 (d, J = 5.3 Hz, 1H), 7.08 (s, 1H), 7.01 (d, J = 5.3 Hz, 1H), 4.29-4.22 (m, 4H), 4.20 (m, J = 12.6, 5.6 Hz, 3H), 1.91-1.84 (m, 2H), 1.37-1.21 (m, 13H), 1.16 (m, J = 7.1 Hz, 7H), 0.87 (t, J = 6.8 Hz, 3H). ^{13}C NMR (125 MHz, $CDCl_3$, δ): 168.50, 168.10,

146.76, 145.08, 144.93, 137.47, 135.33, 134.30, 134.17, 133.96, 132.54, 131.97, 131.77, 129.96, 129.51, 123.93, 116.12, 115.01, 111.21, 111.16, 77.59, 77.33, 77.08, 61.99, 61.91, 47.74, 32.04, 30.65, 29.51, 29.39, 28.52, 27.28, 27.05, 22.86, 17.59, 14.34, 14.21, 14.06, 13.88. MALDI-TOF MS (m/z): $[M+H]^+$ calcd. for $C_{32}H_{35}NO_4S_2Se$, 641.1173; found, 641.1166.

*Synthesis of **DTPPSe**.*

To a stirring solution of 1-bromo-4-hexylbenzene (1.24 g, 5.15 mmol) in dry THF (40 mL) at -78 °C was added dropwise *n*-BuLi (1.89 mL, 4.72 mmol, 2.5 M in hexane) under nitrogen atmosphere and the mixture was kept at -78 °C for 1 h. A solution of compound **2** (550 mg, 0.86 mmol) in dry THF (5 mL) was dropped slowly with a syringe. Then the resulting mixture was warmed to room temperature and stirred overnight. The resulting mixture was poured into water and extracted with ethyl acetate. The combined organic layers were dried over anhydrous $MgSO_4$ and filtered. The filtrate was concentrated under vacuum. Then the crude product was dissolved in petroleum ether/acetic acid (120 mL, 2:1, v/v) and two drops of sulfuric acid are added. After stirring at 60 °C for 30 min, the mixture was poured into water and extracted with petroleum ether. The combined organic layers were dried over anhydrous $MgSO_4$ and filtered. The filtrate was concentrated under vacuum and purified by column chromatography on silica gel with petroleum ether as an eluent to give a light yellow liquid (518 mg, 52%). ^{1}H NMR (500 MHz, $CDCl_3$, δ): 7.84 (d, J = 5.3 Hz, 1H), 7.40 (s, 1H), 7.36 (s, 1H), 7.34 (d, J = 8.2 Hz, 4H), 7.19 (d, J = 5.3 Hz, 1H), 7.16 (d, J = 8.2 Hz, 5H), 7.08 (m, J = 10.5 Hz, 11H), 6.90 (d, J = 5.2 Hz, 1H), 3.76-3.71 (m, 2H), 2.57 (t, J = 7.1 Hz, 9H), 1.63-1.57 (m, 9H), 1.36-1.26 (m, 31H), 1.18 (m, J = 18.8 Hz, 4H), 1.07 (m, J = 17.2 Hz, 2H), 1.01 (m, J = 14.2 Hz, 2H), 0.90-0.88 (m, 12H). ^{13}C NMR (125 MHz, $CDCl_3$, δ): 157.42, 156.44, 152.97, 144.59, 144.50, 142.20, 141.91, 141.55, 140.67, 140.22, 139.93, 139.02, 137.58, 136.15, 131.62, 129.03, 128.50, 128.21, 125.96, 122.83, 117.86, 116.92, 116.35, 115.83, 111.75, 77.53, 77.27, 77.02, 64.07, 62.68, 48.51, 35.83, 35.80, 32.15, 31.98, 31.97, 31.58, 31.54, 30.61, 29.56, 29.55, 29.42, 27.10, 22.91, 22.86, 14.36. MALDI-TOF MS (m/z): $[M+H]^+$ calcd. for $C_{76}H_{91}NS_2Se$, 1161.5758; found, 1161.5767.

Synthesis of ***Compound 3***.

Under the protection of nitrogen atmosphere, the compound **DTPPSe** (518 mg, 0.45 mmol) was dissolved into a mixed solution of 1,2-dichloroethane/N,N-dimethyl-formamide (DMF) (20 mL/3 mL). Then the solution was cooled to 0 °C and $POCl_3$ (0.5 mL) was dropped by syringe. After stirring at 0 °C for 1 h, the solution was heated to 90 °C and reflux overnight. After the solution was cooled to room temperature, the reaction was neutralized by adding a saturated aqueous solution of sodium carbonate, followed by extraction three times with dichloromethane. The combined organic layers were dried over anhydrous $MgSO_4$ and filtered. The filtrate was concentrated under vacuum and purified by column chromatography on silica gel with petroleum ether : ethyl acetate (10:1) as an eluent to give an orange solid (440 mg, 81%). ^{1}H NMR (500 MHz, $CDCl_3$, δ): 9.84 (s, 1H), 9.66 (s, 1H), 7.84 (s, 1H), 7.52 (d, J = 3.7 Hz, 2H), 7.43 (s, 1H), 7.30 (d, J = 8.3 Hz, 4H), 7.11 (m, J = 10.8 Hz, 13H), 3.79-3.73 (m, 2H), 2.59-2.54 (m, 8H), 1.62-1.54 (m, 10H), 1.30 (m, J = 13.1 Hz, 30H), 1.21-1.12 (m, 5H), 1.11-1.04 (m, 2H), 1.00 (m, J = 14.6 Hz, 2H), 0.89-0.86 (m, 12H). ^{13}C NMR (125 MHz, $CDCl_3$, δ): 178.65, 177.42, 152.59, 151.99, 149.06, 148.92, 145.46, 140.04, 138.82, 138.40, 137.04, 136.75, 135.52, 135.03, 134.84, 132.43, 132.30, 131.84, 130.06, 123.34, 123.31, 122.49, 119.24, 114.39, 113.37, 113.12, 111.11, 72.03, 71.99, 71.78, 71.74, 71.53, 71.49, 58.87, 57.32, 43.12, 30.30, 30.27, 26.61, 26.45, 26.43, 26.05, 25.99, 25.17, 24.03, 24.00, 23.90, 23.87, 21.57, 17.39, 17.33, 8.84, 8.83. MALDI-TOF MS (m/z): $[M+H]^+$ calcd. for $C_{78}H_{91}NO_2S_2Se$, 1217.5656; found, 1217.5661.

Synthesis of ***DTPPSe-IC***.

Compound **3** (100 mg, 0.08 mmol), 2-(3-oxo-2,3-dihydro-1H-inden-1-ylidene) malononitrile (88 mg, 0.45 mmol) and β-alanine (2 mg, 0.022 mmol) were dissolved in a mixture solution of 1,2-dichloroethane/absolute ethanol (6 mL/3 mL). Then the solution was heated to 65 °C and stirred overnight. The resulting mixture was recrystallized from methanol and filtered, then the filter residue was rinsed with dichloromethane to a rotary flask. After removing the solvent, the mixture was purified by column chromatography on silica gel with petroleum ether: dichloro-methane (2:1) as an eluent to give a dark solid (90 mg, 70%). ^{1}H NMR (500 MHz,

$CDCl_3$, δ): 8.93 (s, 1H), 8.87 (s, 1H), 8.66-8.63 (m, 1H), 8.63-8.60 (m, 1H), 7.89-7.82 (m, 3H), 7.73-7.67 (m, 2H), 7.64 (t, J = 3.4 Hz, 3H), 7.58 (s, 1H), 7.48 (s, 1H), 7.33 (d, J = 8.3 Hz, 4H), 7.13 (m, J = 16.4 Hz, 12H), 3.79-3.75 (m, 2H), 2.59 (m, J = 16.0 Hz, 8H), 1.65-1.57 (m, 9H), 1.41-1.24 (m, 30H), 1.23-1.16 (m, 4H), 1.14-1.07 (m, 2H), 1.02 (m, J = 14.4 Hz, 2H), 0.89-0.85 (m, 12H). ^{13}C NMR (125 MHz, $CDCl_3$, δ): 183.67, 183.00, 161.09, 155.54, 155.03, 154.25, 152.86, 150.42, 144.58, 141.43, 141.10, 138.07, 138.01, 137.55, 137.37, 136.94, 136.03, 135.22, 135.15, 134.72, 134.54, 133.30, 133.23, 133.12, 131.92, 131.56, 131.53, 131.18, 129.75, 129.32, 129.02, 128.98, 128.70, 128.66, 123.46, 123.42, 123.22, 122.51, 120.37, 119.97, 119.66, 118.37, 118.09, 115.76, 115.17, 114.77, 113.98, 111.77, 110.15, 110.00, 109.50, 109.44, 72.01, 71.96, 71.76, 71.50, 63.37, 61.58, 58.79, 57.34, 43.25, 30.30, 30.27, 26.61, 26.44, 26.42, 26.05, 25.97, 25.17, 24.08, 23.99, 23.90, 23.85, 21.53, 17.39, 17.32, 8.83, 8.81. MALDI-TOF MS (m/z): $[M+H]^+$ calcd. for $C_{102}H_{99}N_5O_2S_2Se$, 1569.6405; found, 1569.6401.

Synthesis of ***DTPPSe-2F***.

Compound **3** (100 mg, 0.08 mmol), 2-(6-fluoro-3-oxo-2,3-dihydro-1H-inden-1-ylidene)malononitrile (96 mg, 0.45 mmol) and β-alanine (2 mg, 0.022 mmol) were dissolved in a mixture solution of 1,2-dichloroethane/absolute ethanol (6 mL/3 mL). Then the solution was heated to 65 °C and stirred overnight. The resulting mixture was recrystallized from methanol and filtered, then the filter residue was rinsed with dichloromethane to a rotary flask. After removing the solvent, the mixture was purified by column chromatography on silica gel with petroleum ether : dichloromethane (2:1) as an eluent to give a dark solid (80 mg, 61%). ^1H NMR (500 MHz, $CDCl_3$, δ): 8.93 (d, J = 5.0 Hz, 1H), 8.84 (s, 1H), 8.68-8.56 (m, 1H), 8.32 (m, J = 23.2 Hz, 1H), 7.89-7.79 (m, 2H), 7.67 (s, 1H), 7.50 (s, 3H), 7.34 (d, J = 7.8 Hz, 4H), 7.26 (s, 2H), 7.19-7.10 (m, 13H), 3.79 (m, 2H), 2.60 (m, J = 15.8 Hz, 8H), 1.61 (m, 9H), 1.44-1.25 (m, 30H), 1.21 (m, J = 4.8 Hz, 4H), 1.13 (m, 2H), 1.04 (m, 2H), 0.89 (m, 12H). ^{13}C NMR (125 MHz, $CDCl_3$, δ): 187.74, 187.06, 167.97, 167.73, 167.35, 167.17, 165.92, 165.69, 159.97, 159.45, 159.09, 158.50, 156.07, 150.59, 147.33, 147.29, 146.79, 143.59, 143.54, 143.38, 142.95, 142.59, 142.52, 142.42, 142.33, 141.75, 141.60, 140.72, 140.65, 138.97, 138.94, 138.80, 138.75, 138.68, 138.58,

137.36, 136.69, 136.04, 136.03, 135.89, 134.80, 133.22, 129.00, 128.97, 128.74, 128.02, 126.12, 126.03, 125.96, 125.66, 125.57, 121.88, 121.69, 121.57, 121.36, 121.18, 121.13, 121.05, 120.46, 120.41, 119.60, 117.41, 115.51, 115.38, 115.10, 115.02, 114.81, 114.65, 114.61, 114.57, 114.55, 113.13, 112.92, 112.85, 112.64, 77.55, 77.30, 77.04, 69.60, 68.68, 67.66, 66.87, 64.32, 62.89, 48.79, 35.82, 35.80, 32.13, 31.97, 31.94, 31.57, 31.49, 30.69, 29.60, 29.51, 29.42, 29.37, 27.05, 22.92, 22.84, 14.36, 14.34. MALDI-TOF MS (m/z): $[M+H]^+$ calcd. for $C_{102}H_{97}F_2N_5O_2S_2Se$, 1605.6217; found, 1605.6214.

Synthesis of ***DTPPSe-4F***.

Compound **3** (100 mg, 0.08 mmol), 2-(6-fluoro-3-oxo-2,3-dihydro-1H-inden-1-ylidene)malononitrile (104 mg, 0.45 mmol) and β-alanine (2 mg, 0.022 mmol) were dissolved in a mixture solution of 1,2-dichloroethane/absolute ethanol (6 mL/3 mL). Then the solution was heated to 65 °C and stirred overnight. The resulting mixture was recrystallized from methanol and filtered, then the filter residue was rinsed with dichloromethane to a rotary flask. After removing the solvent, the mixture was purified by column chromatography on silica gel with petroleum ether/ dichloromethane (1.5:1) as an eluent to give a dark solid (88 mg, 65%). ^{1}H NMR (500 MHz, $CDCl_3$, δ): 8.93 (s, 1H), 8.82 (s, 1H), 8.51 (m, J = 9.8 Hz, 1H), 8.44 (m, J = 9.9 Hz, 1H), 7.87 (s, 1H), 7.69 (s, 1H), 7.65-7.56 (m, 3H), 7.51 (s, 1H), 7.34 (d, J = 8.3 Hz, 4H), 7.19-7.10 (m, 12H), 3.83-3.75 (m, 2H), 2.60 (m, J = 16.2 Hz, 8H), 1.66-1.57 (m, 9H), 1.41-1.25 (m, 30H), 1.25-1.16 (m, 4H), 1.14-1.09 (m, 2H), 1.08-0.99 (m, 2H), 0.90-0.85 (m, 12H). ^{13}C NMR (125 MHz, $CDCl_3$, δ): 181.28, 180.54, 162.26, 154.64, 153.24, 153.10, 152.89, 150.68, 150.22, 150.18, 150.11, 150.07, 149.91, 149.78, 148.15, 148.08, 148.04, 147.97, 147.83, 147.72, 145.49, 142.10, 141.41, 138.20, 137.99, 137.47, 137.05, 136.16, 135.26, 135.05, 133.54, 133.28, 133.01, 131.76, 131.29, 131.27, 131.23, 131.12, 129.57, 129.14, 129.09, 123.50, 123.47, 123.22, 122.49, 115.03, 114.88, 114.20, 111.99, 109.80, 109.71, 109.61, 109.48, 109.31, 109.09, 108.98, 107.37, 107.22, 107.06, 106.92, 72.04, 71.99, 71.79, 71.53, 63.88, 61.97, 58.80, 57.39, 43.29, 30.31, 30.28, 26.62, 26.45, 26.43, 26.05, 25.98, 25.16, 24.09, 23.98, 23.91, 23.86, 21.53, 17.41, 17.33, 8.84, 8.83. MALDI-TOF MS (m/z): $[M+H]^+$ calcd. for $C_{102}H_{95}F_4N_5O_2S_2Se$, 1641.6029; found, 1641.6031.

S1.2 Instruments and general methods

The ^{1}H NMR, ^{13}C NMR spectra were measured using Bruker ADVANCE 500 MHz spectrometer with deuterated chloroform ($CDCl_3$) as the solvent and trimethylsilane (TMS) as the internal reference. Mass spectra were measured using GCT-MS EI and Bruker Daltonics Biflex III MALDI-TOF Analyzer in the MALDI mode. Absorption spectra were taken on a UV-Vis instrument Evolution 220 (Thermo Fisher). The electrochemical cyclic voltammetry (CV) was conducted on an electrochemical workstation (CHI760E Chenhua Shanghai) with Pt plate as working electrode, Pt slice as counter electrode, and Ag/AgCl electrode as reference electrode in tetrabutylammonium hexafluorophosphate (Bu_4NPF_6, 0.1 M) acetonitrile solutions at a scan rate of 100 mV s^{-1}. Ferrocene/ferrocenium (Fc/Fc^+) was used as the internal standard (the energy level of Fc/Fc^+ is -4.8 eV under vacuum), and the formal potential of Fc/Fc^+ was measured as 0.34 V vs. Ag/AgCl electrode. Thermogravimetric analysis (TGA) was conducted under nitrogen atmosphere at a heating rate of 20 °C min^{-1} from 50 °C to 800 °C. The instrument type was TGA/SDTA851E (Mettler Toledo). AFM images were measured on a Bruker Multimode 8 Atomic Force Microscope.

S1.3 Devices fabrication and characterization

All the OSCs devices were fabricated in the inverted structure of indium tin oxide (ITO)/zinc oxide (ZnO)/Active Layers/MoO_3/Ag. The patterned ITO-coated glass substrates were cleaned by sequential ultrasonic treatment in glass detergent, deionized water, acetone, and isopropanol for 15 min each and subsequently dried by oxygen plasma for 90 seconds for further clearance. After drying, a 30 nm layer of sol-gel ZnO was deposited by spin-coating ZnO precursor solution on the cleaned ITO substrates at 4000 rpm for 30 s and then annealed at 180 °C for 30 min. Whereafter, the photovoltaic layers were spin-coated in a glove box with the mixture (10 mg ml^{-1} for polymer) in CB with DIO additive on the top of ZnO layer. MoO_3 (8 nm) and Ag (150 nm) layers were successively deposited by thermal evaporation. The effective area for the OSCs devices is 3.97 mm^2. The current-Voltage characteristics of all OSCs devices were measured by a Keithley 2400 source meter under a Newport

solar simulator calibrated to 1 sun, AM 1.5G. The external quantum efficiency (EQE) spectra of inverted devices were obtained using a Solar Cell Spectral Response Measurement System QE-R3011 (Enlitech Co., Ltd.). The light intensity at each wavelength was also calibrated using a standard single crystal Si photovoltaic cell. The film thicknesseses were measured using Bruker DektakXT stylus profiling system.

S1.4 Space-Charge Limited Current (SCLC) Measurement

Charge carrier mobilities were tested using the diode configuration of ITO/ZnO/active layer/PDINO/Al for electron and ITO/PEDOT:PSS/active layer/MoO_3/Ag for hole via the SCLC method, which described by $J=9\varepsilon_0\varepsilon_r\mu V^2/8L^3$. J is the current density, L is the film thickness of the active layer, μ is the hole or electron mobility, ε_r is the relative dielectric constant of the transport medium, ε_0 is the permittivity of free space (8.85×10^{-12} F m^{-1}), V (= V_{appl} - V_{bi}) is the internal voltage in the device, where V_{appl} is the applied voltage to the device and V_{bi} is the built-in voltage due to the relative work function difference of the two electrodes.

S2. Figures and Tables

Table S1 Comparison of device parameters for all selenophene-containing FRAs-based OSCs.

Active Layer	V_{OC} (V)	J_{SC} (mA cm^{-2})	FF (%)	PCE (%)	Ref.
PBDB-T:DTPPSe-2F	**0.84**	**22.16**	**73.70**	**13.76**	**This work**
PM6:TSeTIC	0.93	19.42	75.90	13.71	[2]
PM6:SeTIC4Cl	0.78	22.92	75.00	13.32	[3]
PBDB-T-2F:SRID-4F	0.85	20.21	75.20	13.05	[4]
PBDB-T-2F:TRID-4F	0.89	18.45	75.00	12.33	[4]
PBT1-C:SePTTT-2F	0.90	18.02	75.90	12.24	[5]
PBDB-T:DTPPSe-4F	**0.78**	**21.18**	**72.84**	**12.03**	**This work**
PBDB-T:IDT2Se-4F	0.79	21.49	65.90	11.19	[6]
PBT1-C:SePTT-2F	0.83	17.51	75.00	10.90	[5]
PBDB-T:IDTO-Se-4F	0.83	18.55	69.20	10.67	[7]
PBT1-C:SePT-IN	0.85	16.37	73.30	10.20	[8]
PBDB-T:DTPPSe-IC	**0.90**	**17.32**	**63.36**	**9.88**	**This work**
PBDB-T:STIC	0.77	19.96	63.00	9.68	[9]

PBDB-T:IDT2Se	0.89	17.49	60.80	9.36	[6]
PBDB-T:ITCPTC-Se	0.87	15.20	68.30	9.02	[10]
J51:IDSe-T-IC	0.91	15.20	62.00	8.58	[11]
PDBT-T1:SdiPBI-Se	0.96	12.49	70.20	8.42	[12]
J51:IDTIDSe-IC	0.91	15.16	58.00	8.02	[13]
PM6:SeTIC	0.95	15.45	51.00	7.46	[3]
PBT7-Th:FPDI-Se	0.80	14.78	56.10	6.61	[14]

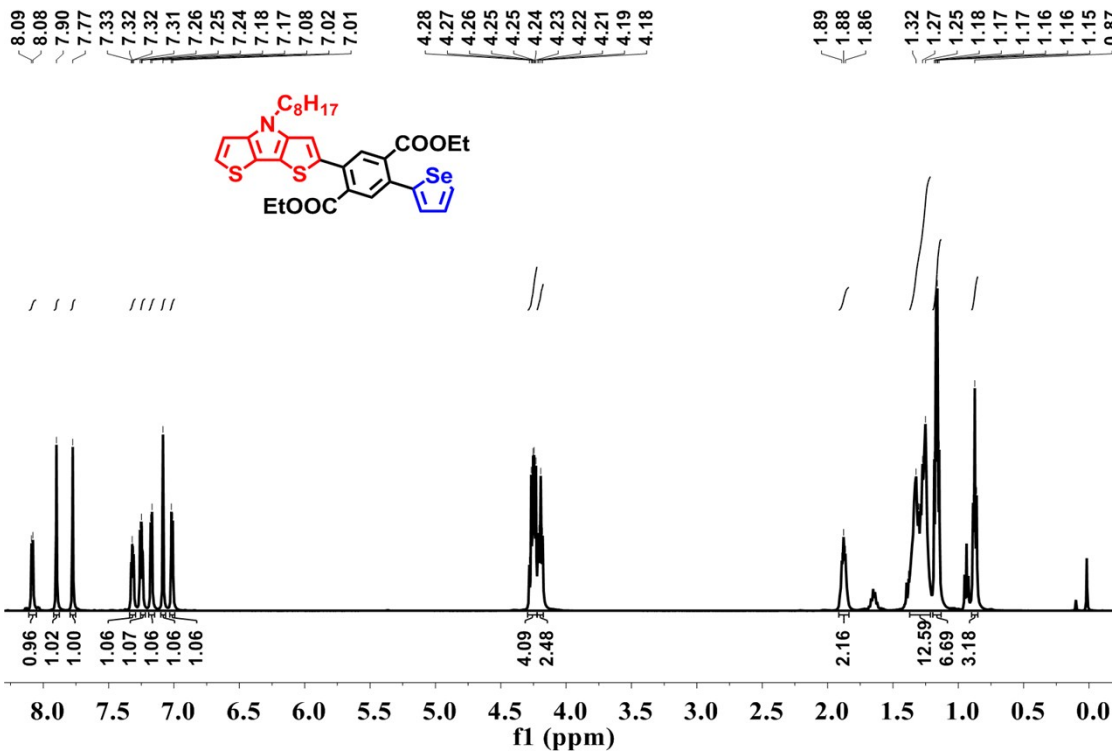

Fig. S1 ^{1}H NMR spectrum of **compound 2**.

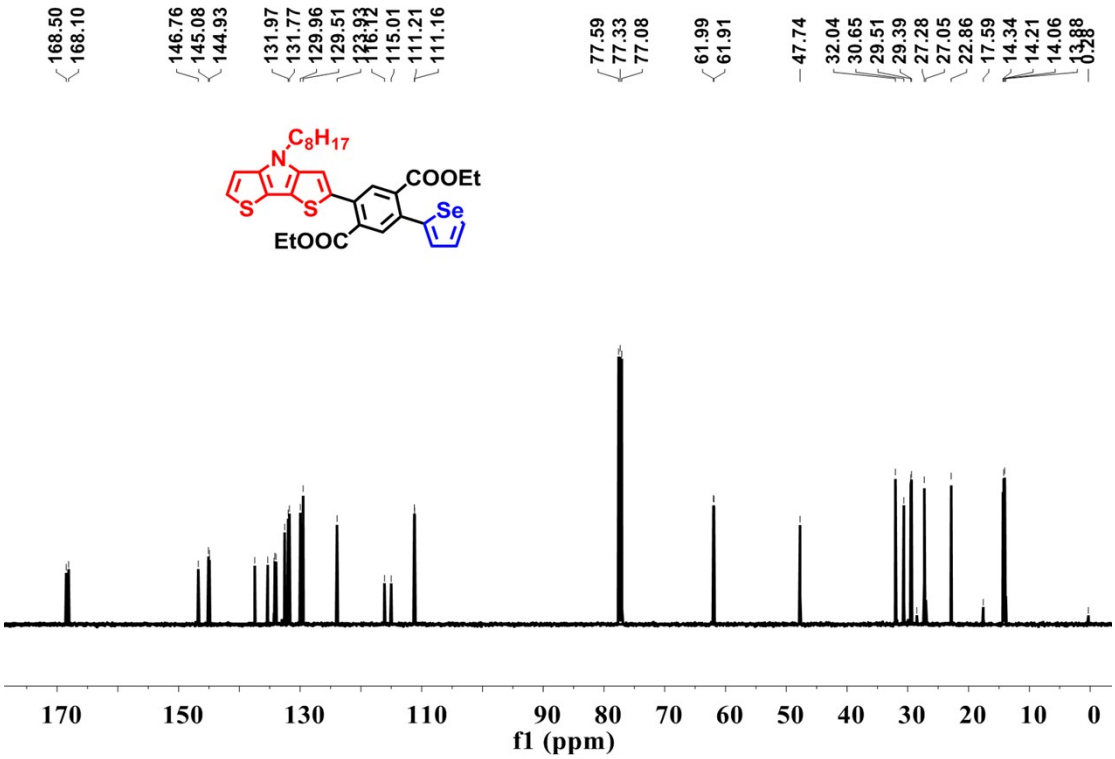

Fig. S2 ^{13}C NMR spectrum of **compound 2**.

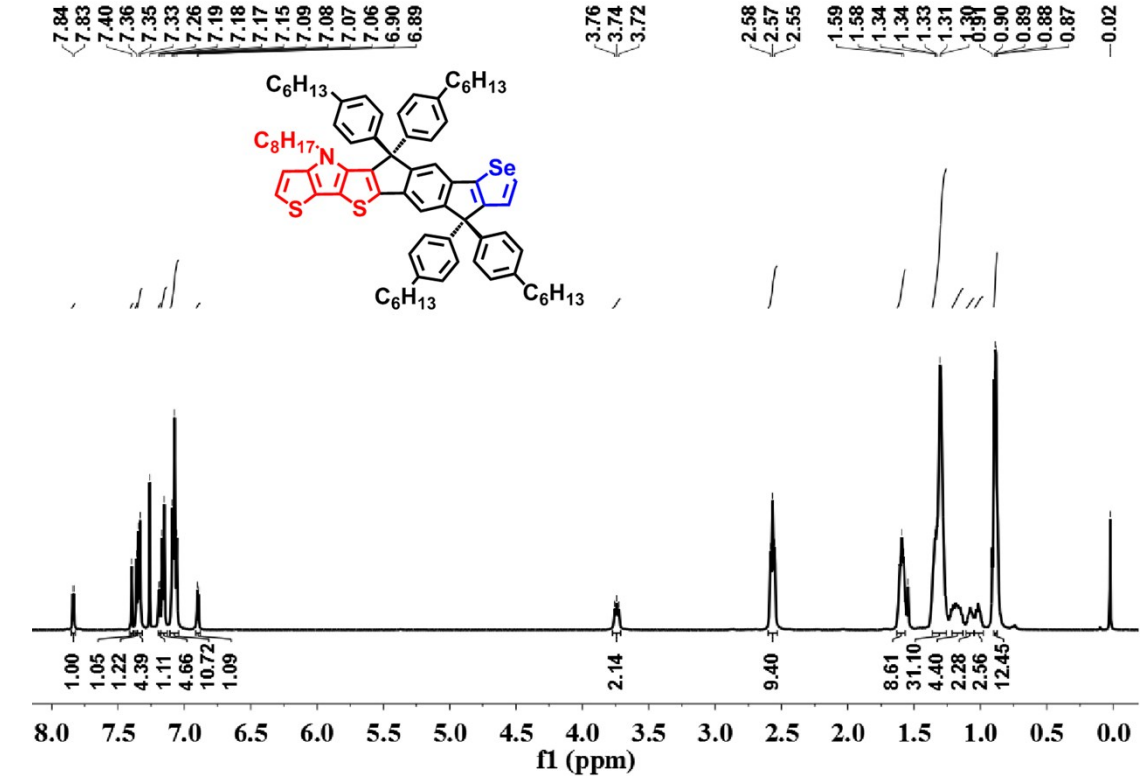

Fig. S3 ^{1}H NMR spectrum of **DTPPSe**.

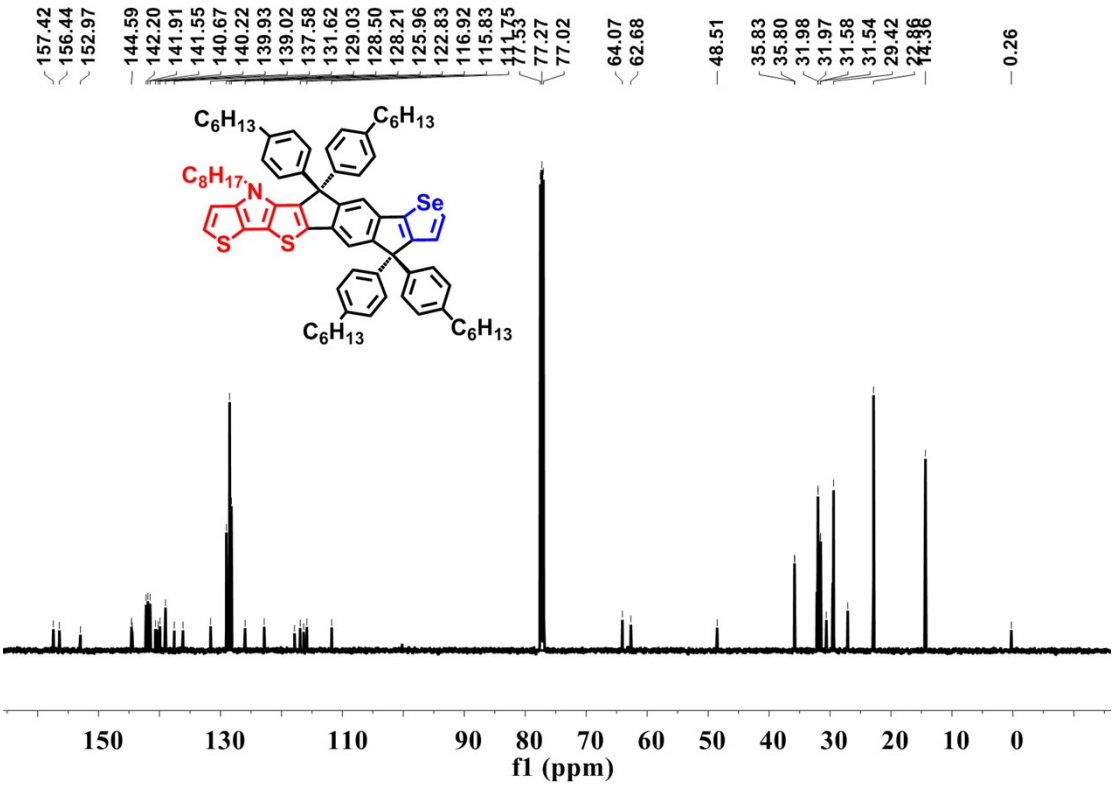

Fig. S4 ^{13}C NMR spectrum of **DTPPSe**.

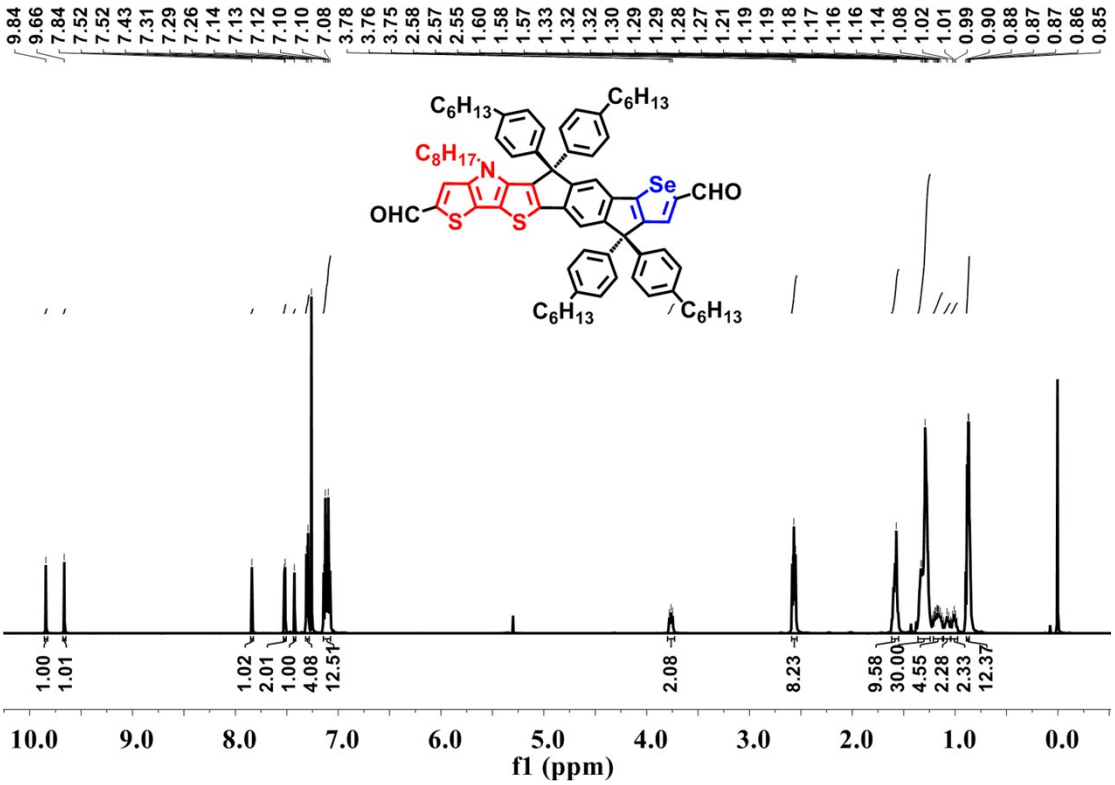

Fig. S5 ^{1}H NMR spectrum of **compound 3**.

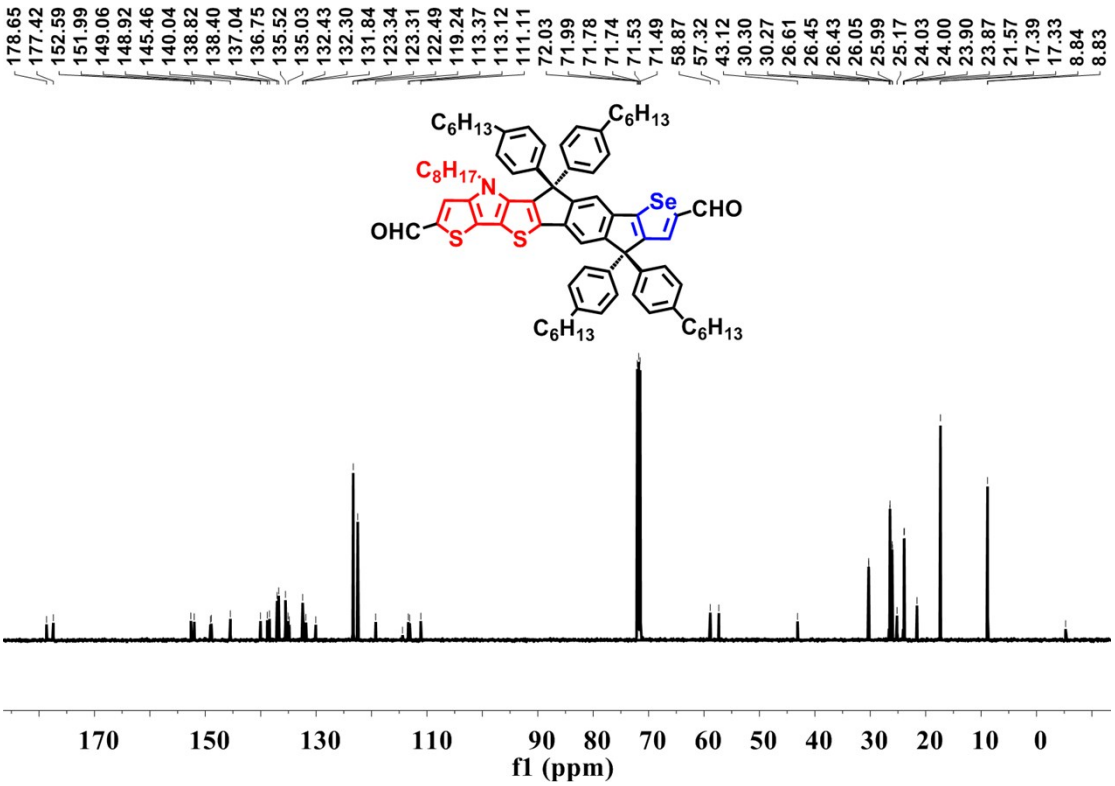

Fig. S6 ^{13}C NMR spectrum of **compound 3**.

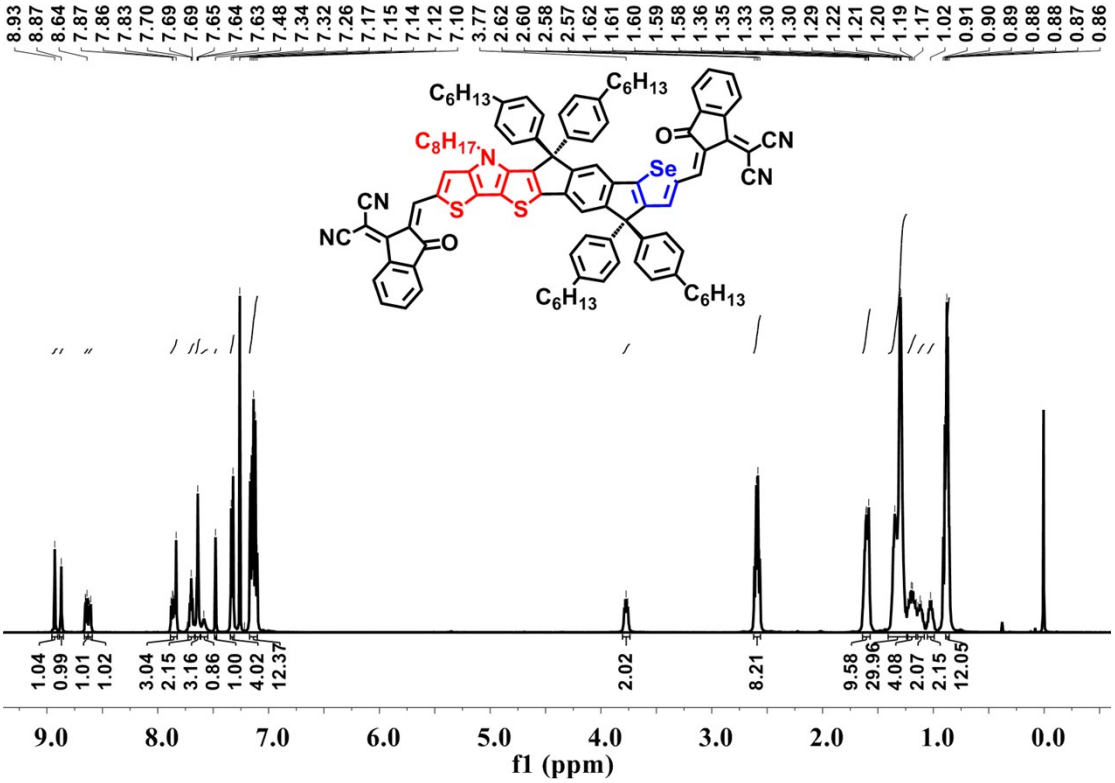

Fig. S7 ^{1}H NMR spectrum of **DTPPSe-IC**.

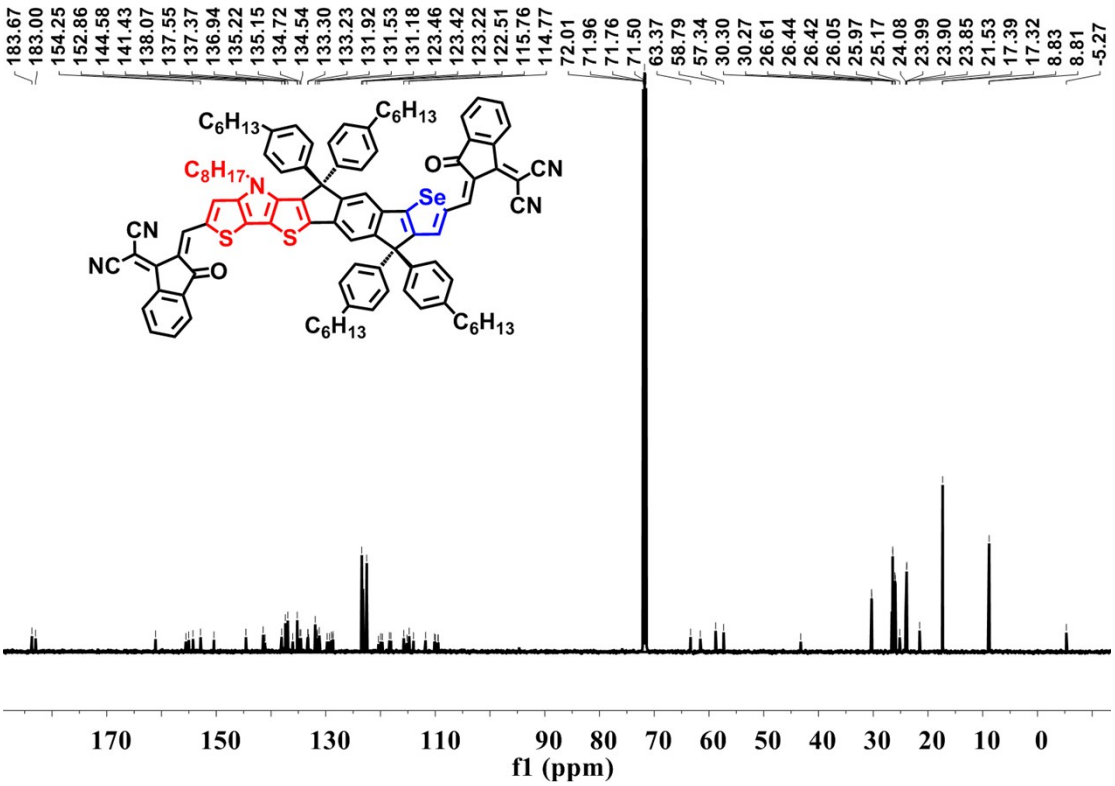

Fig. S8 ^{13}C NMR spectrum of **DTPPSe-IC**.

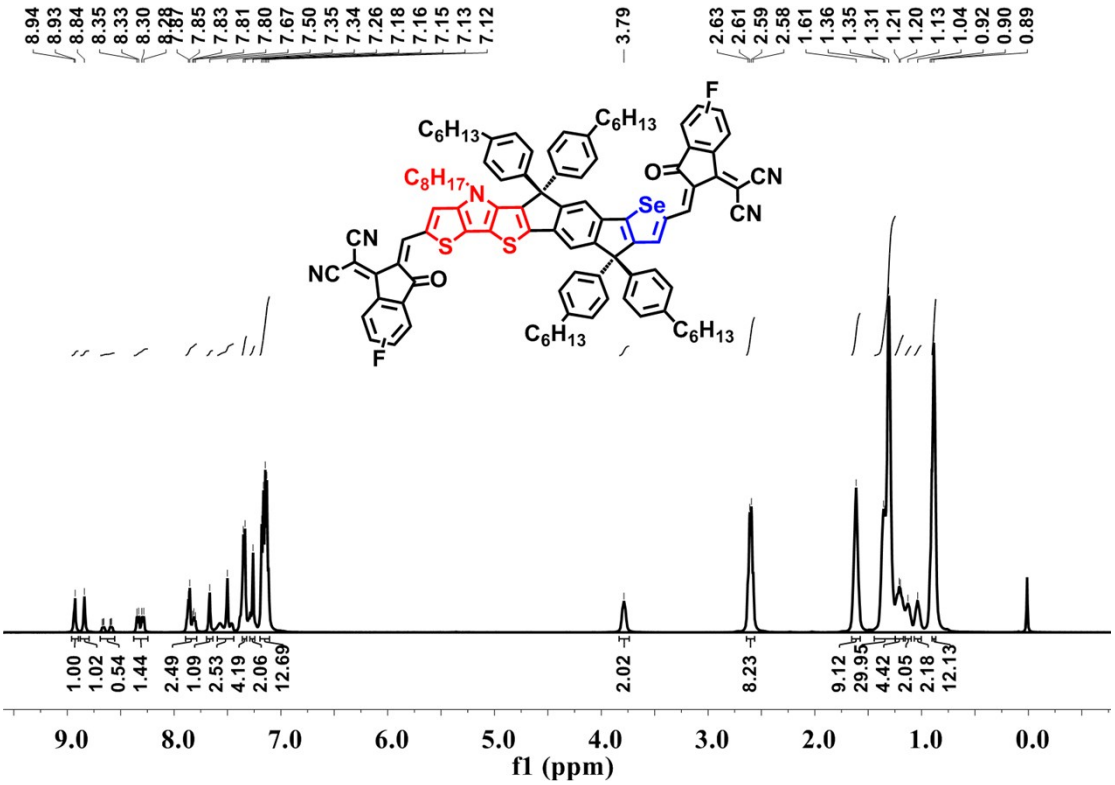

Fig. S9 ^{1}H NMR spectrum of **DTPPSe-2F**.

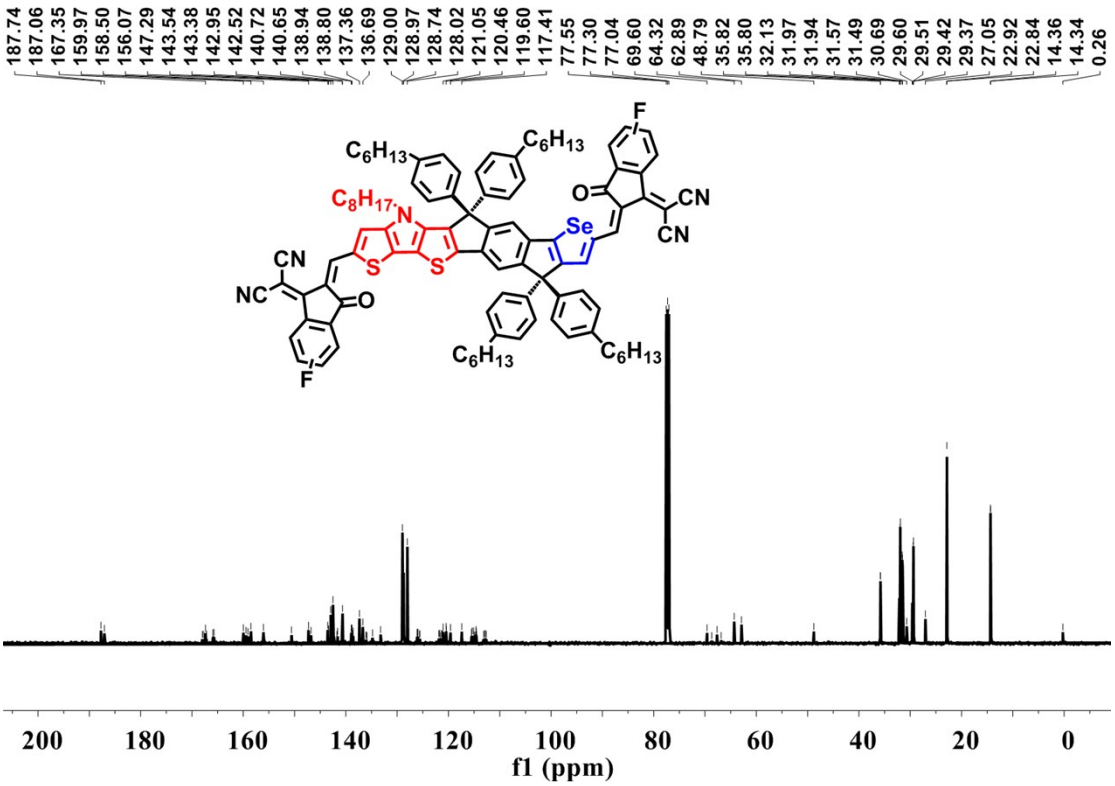

Fig. S10 ^{13}C NMR spectrum of **DTPPSe-2F**.

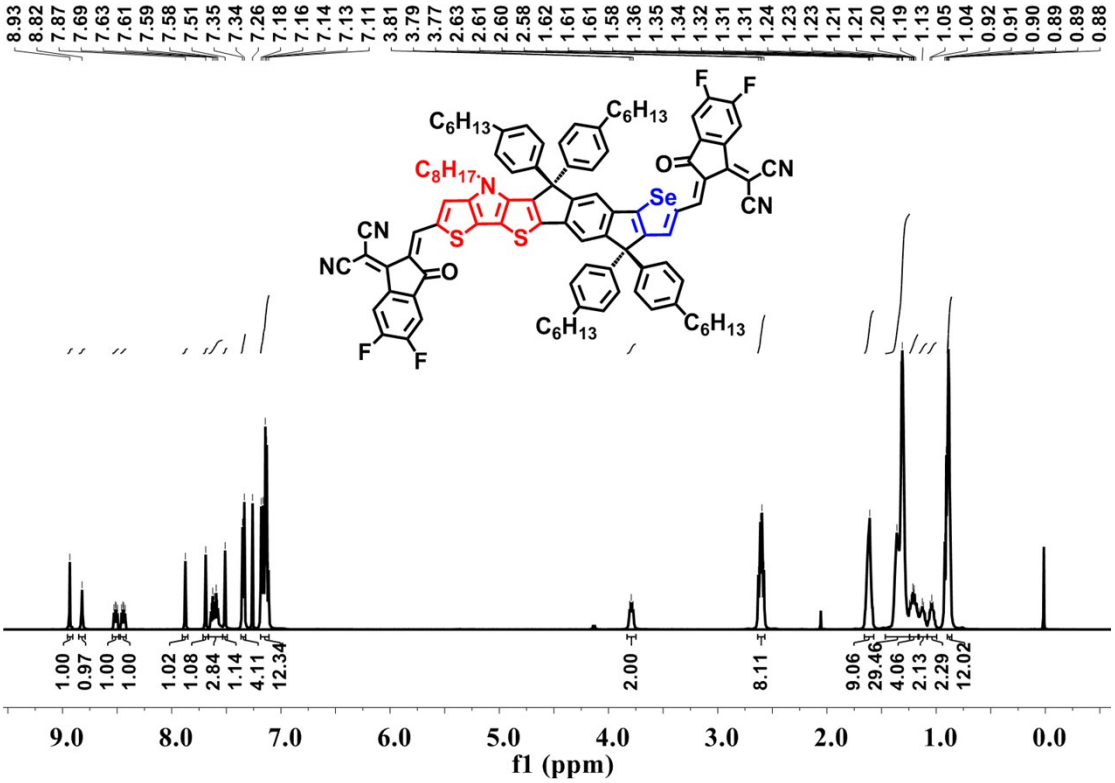

Fig. S11 ^{1}H NMR spectrum of **DTPPSe-4F**.

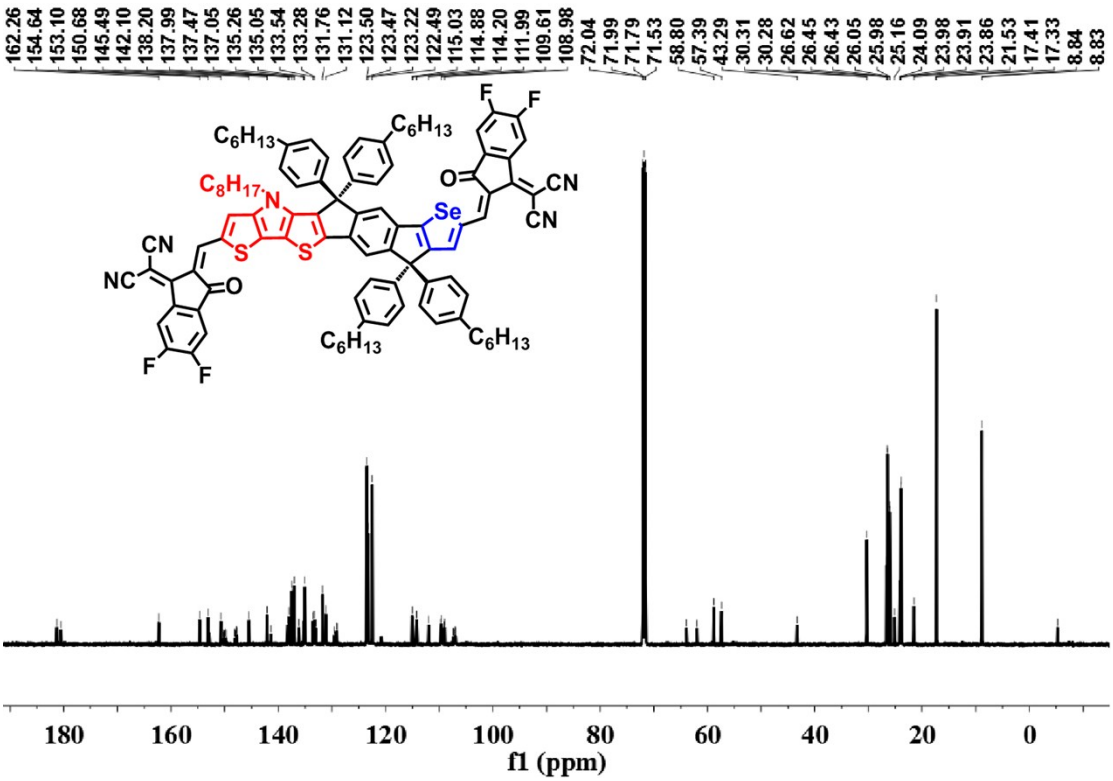

Fig. S12 ^{13}C NMR spectrum of **DTPPSe-4F**.

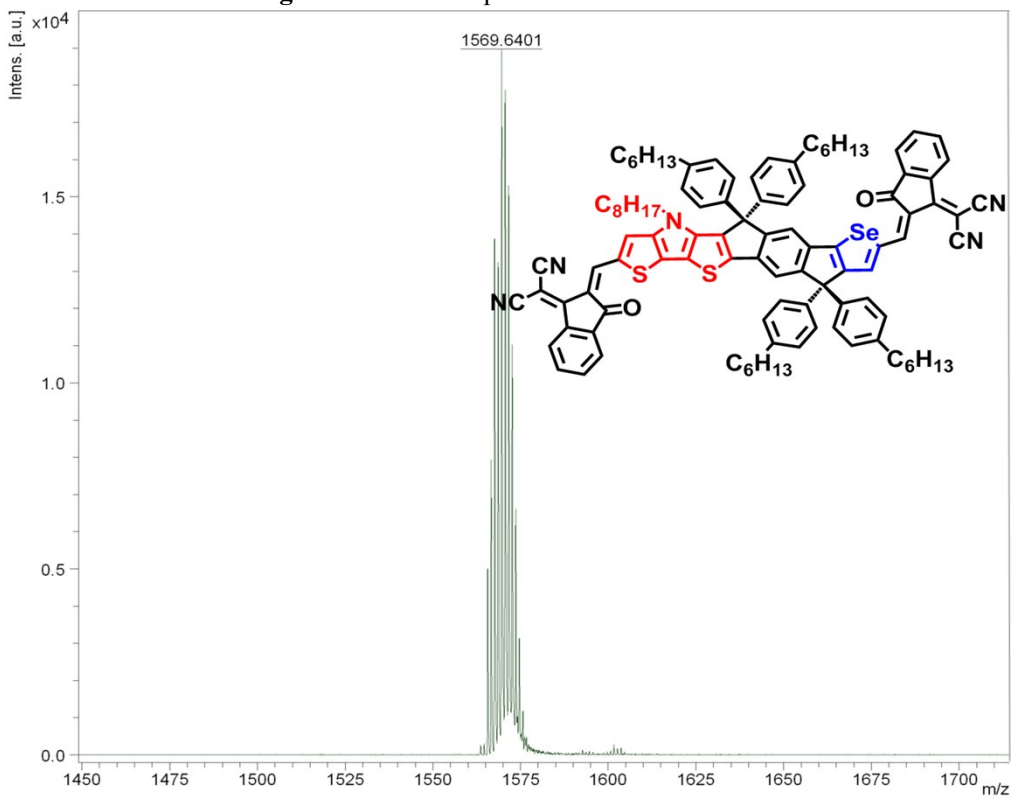

Fig. S13 The MALDI-TOF MS plots of **DTPPSe-IC**.

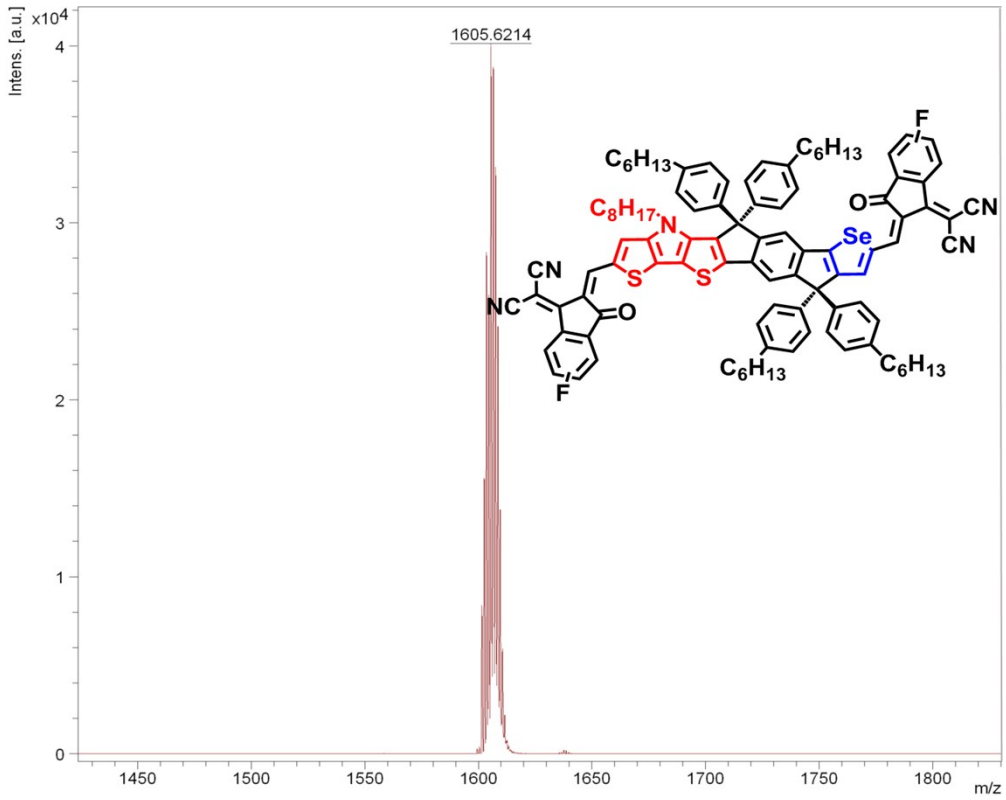

Fig. S14 The MALDI-TOF MS plots of **DTPPSe-2F**.

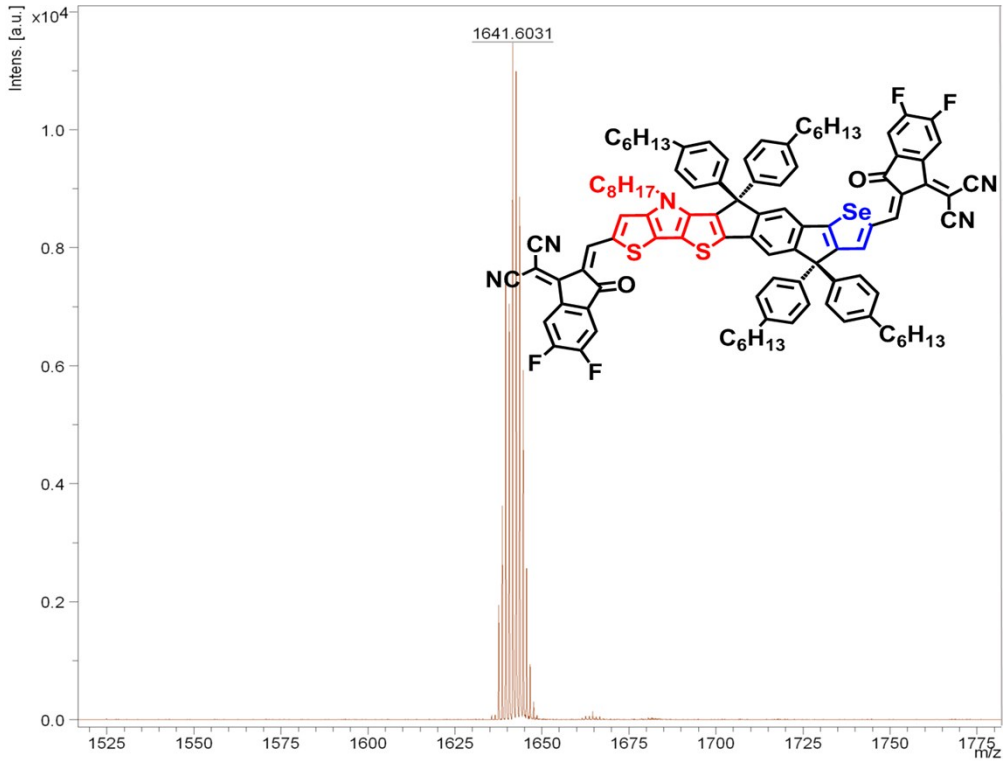

Fig. S15 The MALDI-TOF MS plots of **DTPPSe-4F**.

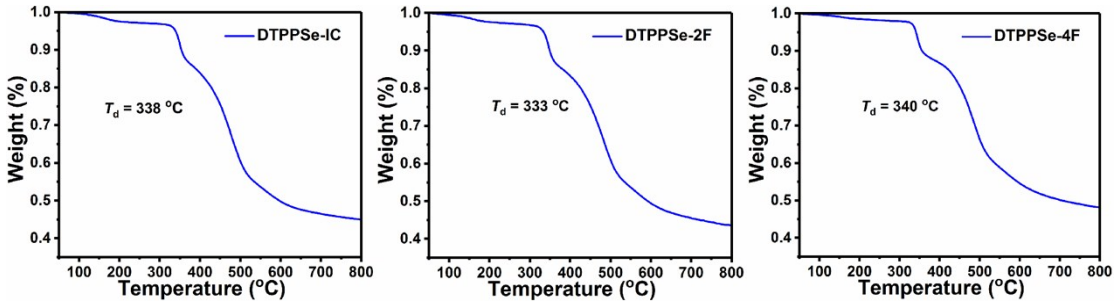

Fig. S16 TGA measurements of DTPPSe-based FRAs with a ramping rate of 20 °C/min.

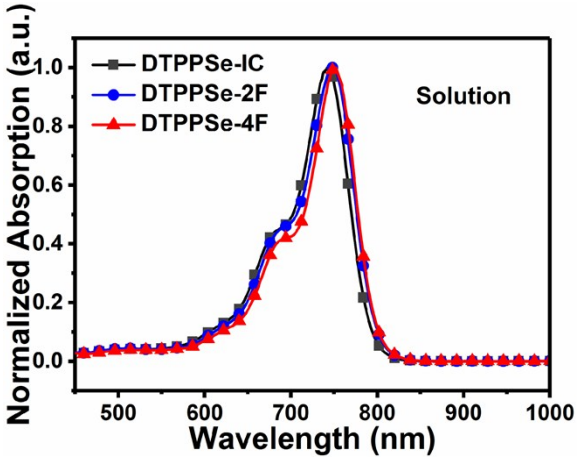

Fig. S17 Normalized absorption spectra of DTPPSe-based FRAs in chloroform (CF) solution.

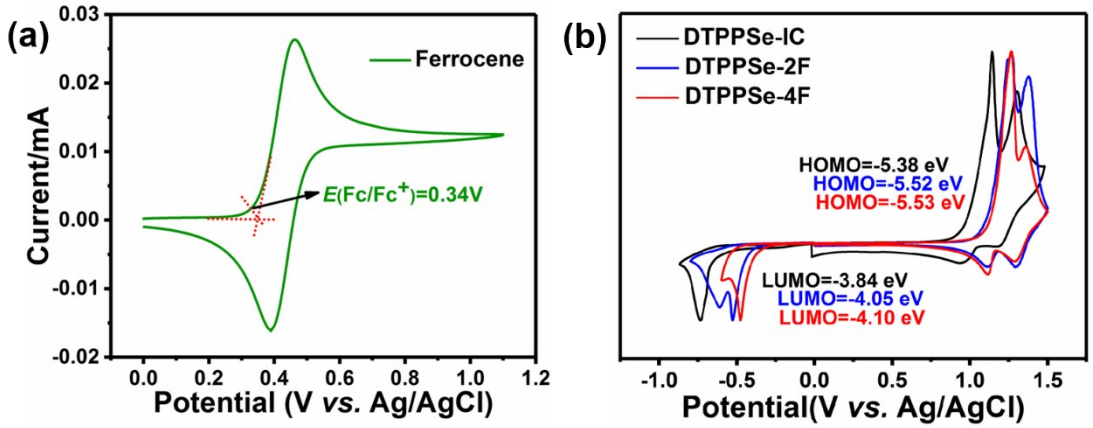

Fig. S18 Cyclic voltammograms of (a) ferrocene external standard and (b) DTPPSe-based FRAs.

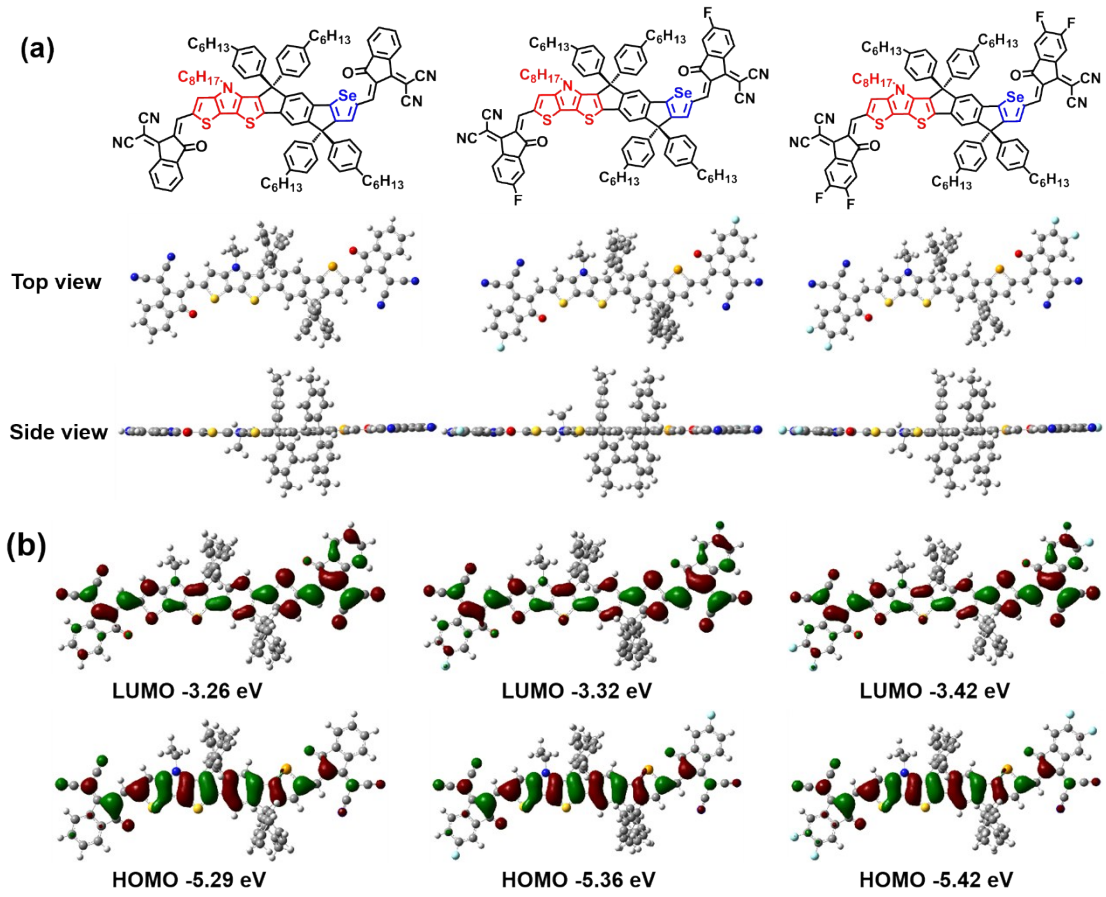

Fig. S19 (a) The top and side view and (b) The LUMO and HOMO distribution of DTPPSe-based FRAs.

Table S2 The optimized photovoltaic parameters of devices based on PBDB-T:FRAs with different D/A ratios.

Active layer	D/A	V_{OC}(V)	J_{SC}(mA cm^{-2})	FF (%)	PCE[a] (%)
PBDB-T:DTPPSe-IC	1:1	0.90 (0.89±0.01)	13.87 (13.62±0.18)	62.65 (62.57±0.36)	7.82 (7.70±0.09)
	1:1.25	**0.91 (0.89±0.02)**	**16.79 (16.65±0.11)**	**62.71 (62.18±0.56)**	**9.36 (9.16±0.21)**
	1:1.5	0.89 (0.89±0.00)	13.20 (13.17±0.12)	61.10 (60.95±0.66)	7.18 (7.11±0.13)
PBDB-T:DTPPSe-	1:1	0.84 (0.84±0.00)	20.06 (20.02±0.25)	61.84 (61.28±0.73)	10.42 (10.30±0.25)

2F

	1.25:1	**0.83 (0.82±0.01)**	**21.18 (21.13±0.14)**	**62.82 (61.80±1.03)**	**11.04 (10.70±0.31)**
	1.5:1	0.82 (0.82±0.00)	20.23 (20.56±0.52)	64.46 (49.65±0.99)	10.69 (8.47±0.38)
PBDB-T:DTPPSe-4F	1:1	0.75 (0.75±0.00)	20.39 (20.21±0.13)	61.70 (61.36±0.49)	9.42 (9.30±0.11)
	1.25:1	**0.78 (0.77±0.01)**	**20.86 (20.74±0.16)**	**68.84 (67.47±1.58)**	**11.20 (10.97±0.22)**
	1.5:1	0.80 (0.80±0.00)	20.50 (20.20±0.22)	58.88 (58.22±0.48)	9.66 (9.41±0.18)

[a] The average values were obtained from over 12 devices.

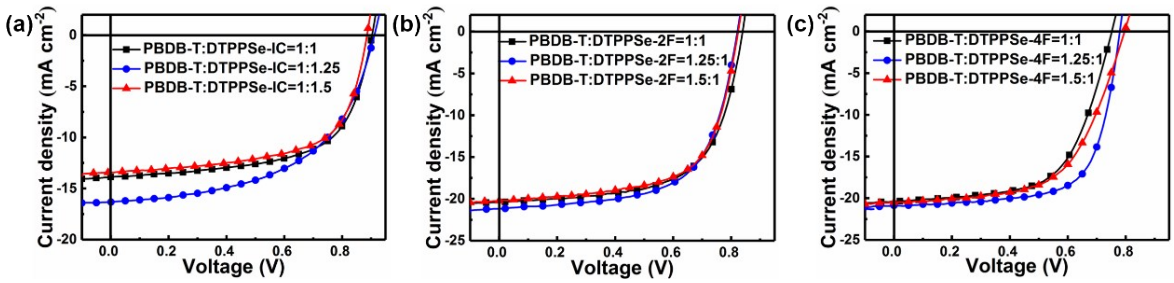

Fig. S20 *J-V* curves of (a) PBDB-T:DTPPSe-IC, (b) PBDB-T:DTPPSe-2F, (c) PBDB-T:DTPPSe-4F based devices with different D/A ratios.

Table S3 The optimized photovoltaic parameters of devices based on PBDB-T:FRAs with different volume ratio additives under optimal D/A ratios.

Active layer	Additives	V_{OC}(V)	J_{SC}(mA cm^{-2})	FF	PCE[a] (%)

				(%)	
PBDB-T:DTPPSe-IC	**None**	**0.91 (0.89±0.02)**	**16.79 (16.65±0.11)**	**62.71 (62.18±0.56)**	**9.36 (9.16±0.21)**
	0.5%DIO	0.89 (0.89±0.00)	17.10 (17.02±0.16)	60.28 (60.02±0.19)	9.18 (9.13±0.05)
	1%DIO	0.91 (0.91±0.00)	16.50 (16.39±0.13)	60.92 (60.89±0.18)	9.15 (9.08±0.06)
PBDB-T:DTPPSe-2F	0.5%DIO	0.84 (0.83±0.01)	21.86 (21.76±0.06)	68.91 (68.38±0.45)	12.61 (12.51±0.07)
	1%DIO	**0.85 (0.84±0.01)**	**22.75 (22.55±0.13)**	**68.60 (68.41±0.16)**	**13.30 (13.23±0.11)**
	2%DIO	0.83 (0.83±0.00)	20.37 (20.08±0.27)	70.05 (69.55±0.68)	11.84 (11.59±0.27)
PBDB-T:DTPPSe-4F	0.5%DIO	0.79 (0.79±0.00)	20.52 (20.42±0.14)	68.52 (68.41±0.15)	11.11 (11.04±0.07)
	1%DIO	**0.78 (0.78±0.00)**	**21.18 (21.05±0.16)**	**72.84 (72.54±0.38)**	**12.03 (11.72±0.28)**
	2%DIO	0.76 (0.76±0.00)	20.93 (20.74±0.37)	67.56 (66.94±0.44)	10.75 (10.55±0.23)

[a] The average values were obtained from over 12 devices.

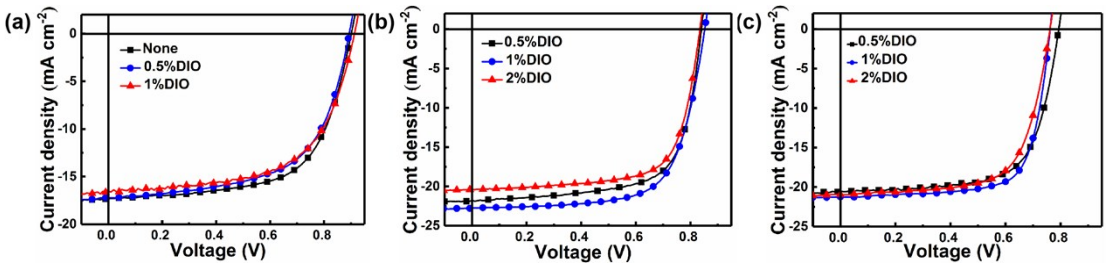

Fig. S21 (a) *J-V* curves of PBDB-T:DTPPSe-IC with different volume ratio additives under optimal D/A ratio of 1:1.25. (b) *J-V* curves of PBDB-T:DTPPSe-2F with different volume ratio additives under optimal D/A ratio of 1.25:1. (c) *J-V* curves of PBDB-T:DTPPSe-4F with different volume ratio additives under optimal D/A ratio of 1.25:1.

Table S4 The optimized photovoltaic parameters of devices based on PBDB-T:FRAs with Different heat treatment temperatures at optimal D/A ratios and additive ratios.

Active layer	Annealing Temperature (°C)	V_{OC}(V)	J_{SC}(mA cm^{-2})	FF (%)	PCE[a] (%)
PBDB-T:DTPPSe-IC	Without	0.91 (0.89±0.01)	16.79 (16.65±0.11)	62.71 (62.18±0.56)	9.36 (9.16±0.21)
	110	**0.90 (0.89±0.01)**	**17.32 (17.02±0.16)**	**63.36 (62.38±0.66)**	**9.88 (9.51±0.07)**
	135	0.91 (0.89±0.01)	17.02 (16.95±0.11)	60.45 (60.18±0.56)	9.36 (9.19±0.18)
PBDB-T:DTPPSe-	Without	0.85 (0.84±0.01)	22.75 (22.55±0.13)	68.60 (68.41±0.16)	13.30 (13.23±0.11)
	110	**0.84 (0.84±0.00)**	**22.16 (22.05±0.16)**	**73.70 (72.74±0.68)**	**13.76 (13.72±0.08)**
	135	0.84 (0.84±0.00)	22.33 (22.12±0.23)	72.14 (71.95±0.26)	13.49 (13.42±0.07)

2F

PBDB-T:DTPPSe-	Without	0.78 (0.78±0.00)	21.18 (21.05±0.16)	72.84 (72.54±0.38)	12.03 (11.72±0.28)
	110	0.75 (0.75±0.00)	20.51 (20.39±0.13)	69.28 (68.87±0.25)	10.66 (10.34±0.27)
	135	0.74 (0.73±0.01)	20.83 (20.75±0.14)	63.89 (63.44±0.45)	9.85 (9.74±0.09)
4F					

[a] The average values were obtained from over 12 devices.

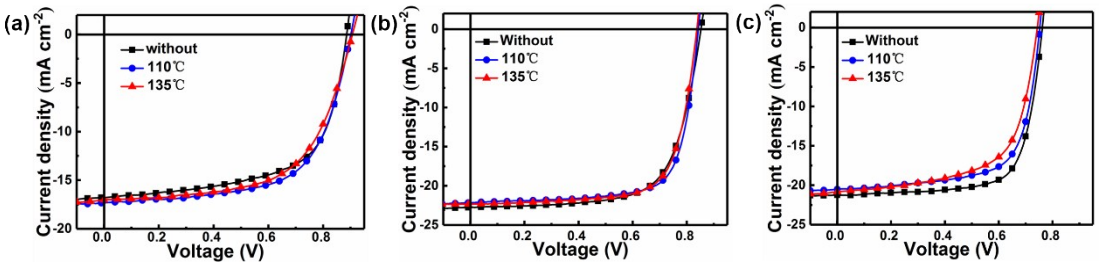

Fig. S22 (a) *J-V* curves of PBDB-T:DTPPSe-IC with different annealing temperature under optimal D/A ratio of 1:1.25. (b) *J-V* curves of PBDB-T:DTPPSe-2F with annealing temperature under optimal D/A ratio of 1.25:1 and 1% DIO. (c) *J-V* curves of PBDB-T:DTPPSe-4F with annealing temperature under optimal D/A ratio of 1.25:1 and 1% DIO.

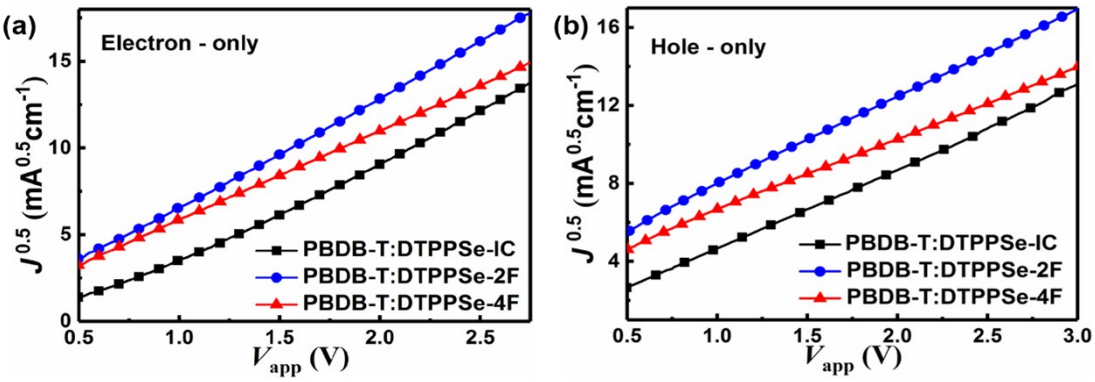

Fig. S23 $J^{0.5}$-V characteristics were acquired from (a) electron-only and (b) hole-only devices with DTPPSe-based FRAs blend films.

Table S5 The optimized photovoltaic parameters of devices based on PBDB-T:FRAs with Different heat treatment temperatures at optimal D/A ratios and additive ratios.

Blend Film	μ_e (cm^2 V^{-1} s^{-1})	μ_h (cm^2 V^{-1} s^{-1})	μ_e/μ_h
PBDB-T:DTPPSe-IC	4.53×10^{-4}	2.48×10^{-4}	1.82
PBDB-T:DTPPSe-2F	5.12×10^{-4}	4.74×10^{-4}	1.08
PBDB-T:DTPPSe-4F	4.96×10^{-4}	4.23×10^{-4}	1.17

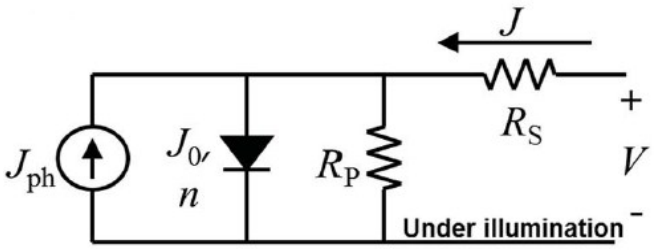

Fig. S24 Circuit diagram of dark current curve measurement.

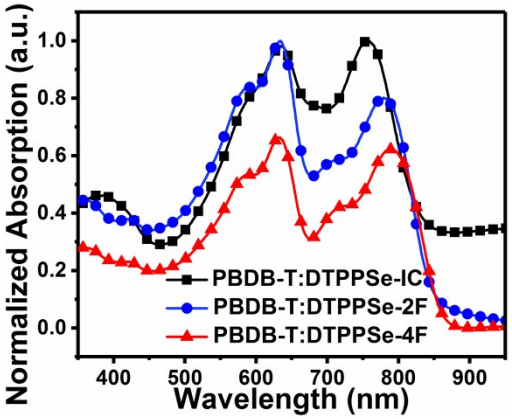

Fig. S25 Normalized absorption spectra of three blend films.

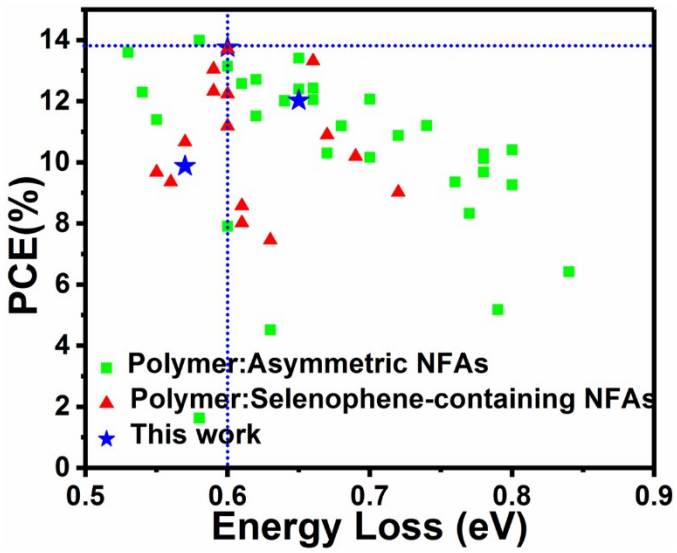

Fig. S26 E_{loss} *vs.* PCE distribution of recent high performance OSCs based on some asymmetric FRAs and selenophene-containing FRAs. The data in the figure is from the Table S6 in the ESI†.

Table S6 E_{loss} *vs.* PCE distribution of recent high performance OSCs based on asymmetric FRAs and selenophene-containing FRAs.

Active Layer	V_{oc} (V)	J_{sc} (mA cm^{-2})	FF (%)	PCE (%)	E_g^{opt} (eV)	E_{loss} (eV)	Ref.
PBDB-T:a-BTTIC	0.90	20.31	74.00	13.60	1.43	0.53	[15]
PBDB-T:IPTTT-2F	0.89	19.20	69.30	12.30	1.43	0.54	[1]
PBDB-T:IPTT-2F	0.87	19.00	66.20	11.40	1.42	0.55	[1]
PBDB-T:STIC	0.77	19.96	63.00	9.68	1.32	0.55	[9]
PBDB-T:IDT2Se	0.89	17.49	60.80	9.36	1.45	0.56	[6]
PBDB-T:DTPPSe-IC	**0.90**	**17.32**	**63.36**	**9.88**	**1.46**	**0.57[a]**	**This work**
PBDB-T:IDTO-Se-4F	0.83	18.55	69.20	10.67	1.40	0.57	[7]
PBDB-T:IPT-2F	0.86	21.20	72.40	14.00	1.44	0.58	[1]
J71:A1	0.97	5.71	29.57	1.63	1.55	0.58	[16]
PBDB-T-2F:SRID-4F	0.85	20.21	75.20	13.05	1.44	0.59	[4]
PBDB-T-2F:TRID-4F	0.89	18.45	75.00	12.33	1.48	0.59	[4]
PBDB-T:DTPPSe-2F	**0.84**	**22.16**	**73.70**	**13.76**	**1.40**	**0.60[a]**	**This work**
PM6:TSeTIC	0.93	19.42	75.90	13.71	1.53	0.60	[2]
PBDB-T:IDT2Se-4F	0.79	21.49	65.90	11.19	1.39	0.60	[6]
J71:ZITI-3F	0.90	20.67	71.53	13.15	1.50	0.60	[17]
PBT1-C:SePTTT-2F	0.90	18.02	75.90	12.24	1.50	0.60	[5]
PBT1-C:TTPTTT-IC	1.00	12.47	63.70	7.91	1.60	0.60	[18]
PBDB-T:MeIC1	0.93	18.32	74.10	12.58	1.54	0.61	[19]
J51:IDSe-T-IC	0.91	15.20	62.00	8.58	1.52	0.61	[11]
J51:IDTIDSe-IC	0.91	15.16	58.00	8.02	1.52	0.61	[13]

PBT1-C:TTPT-T-2F	0.92	18.50	75.10	12.71	1.54	0.62	[20]
PBT1-C:TTPTTT-2F	0.92	16.78	74.60	11.52	1.54	0.62	[18]
J71:A2	0.98	11.63	39.63	4.52	1.61	0.63	[16]
PM6:SeTIC	0.95	15.45	51.00	7.46	1.58	0.63	[3]
PBT1-C-2Cl:IDTT-2F-Th	0.91	17.82	73.90	12.01	1.55	0.64	[21]
PBT1-C:TPTTT-2F	0.92	17.63	74.50	12.03	1.56	0.64	[22]
PBDB-T:DTPPSe-4F	**0.78**	**21.18**	**72.84**	**12.03**	**1.39**	**0.65[a]**	**This work**
PBDB-TF:IT-3F	0.90	20.02	73.30	13.41	1.55	0.65	[23]
PM6:IDT6CN-TM	0.95	17.40	74.70	12.40	1.60	0.65	[24]
PM6:SeTIC-4Cl	0.78	22.92	75.00	13.32	1.44	0.66	[3]
PBDB-T:IDT8CN-M	0.92	17.11	78.90	12.43	1.58	0.66	[25]
PBT1-C:TTPTTT-4F	0.86	19.36	72.10	12.05	1.52	0.66	[18]
PBT1-C:TPTT-IC	0.96	15.50	69.40	10.30	1.63	0.67	[26]
PBT1-C:SePTT-2F	0.83	17.51	75.00	10.90	1.50	0.67	[5]
PBDB-T:IDTT-OB	0.91	16.19	74.00	11.19	1.59	0.68	[27]
PBT1-C:SePT-IN	0.85	16.37	73.30	10.20	1.54	0.69	[8]
PBDB-T:a-IT-2OM	0.93	18.11	71.52	12.07	1.63	0.70	[28]
PBT1-C:TPTT-2F	0.88	15.82	73.00	10.17	1.58	0.70	[22]
PM6:IDT6CN-4F	0.86	18.34	69.10	10.88	1.58	0.72	[24]
PBDB-T:ITCPTC-Se	0.87	15.20	68.30	9.02	1.59	0.72	[10]
PBDB-T:IDT6CN-M	0.91	16.02	76.83	11.20	1.65	0.74	[29]
J71:A201	0.88	13.15	67.15	9.36	1.64	0.76	[30]
PBT1-C:TPT-2F	0.87	13.89	68.60	8.33	1.64	0.77	[22]
PBDB-T:IDT-OB	0.88	16.18	71.10	10.12	1.66	0.78	[31]
PBDB-T:IDT-2O	0.86	15.64	72.30	9.68	1.64	0.78	[31]
PBDB-T:a-IT-2F	0.78	19.06	68.84	10.28	1.56	0.78	[28]
J71:ITCNTC	0.95	11.14	49.20	5.18	1.74	0.79	[32]
PBDB-T:IDT6CN	0.83	15.14	73.77	9.27	1.63	0.80	[29]
PBDB-T:IDT6CN-Th	0.81	16.75	76.72	10.41	1.61	0.80	[29]
PBDB-T:IDT-2B	0.89	13.30	53.90	6.42	1.73	0.84	[31]

[a] The data is calculated by using the absorption onset of blended films.

Reference

1. L. Yang, X. Song, J. Yu, H. Wang, Z. Zhang, R. Geng, J. Cao, D. Baran and W. Tang, *J. Mater. Chem. A*, 2019, **7**, 22279-22286.
2. J.-L. Wang, K.-K. Liu, X. Xu, C. Zhang, G.-Y. Ge, F.-D. Zhuang, H.-J. Zhang, C. Yang, Q. Peng and J. Pei, *J. Mater. Chem. A*, 2019, DOI: 10.1039/c9ta08328f.
3. J.-L. Wang, K.-K. Liu, L. Hong, G.-Y. Ge, C. Zhang and J. Hou, *ACS Energy Lett.*, 2018, **3**, 2967-2976.
4. F. Lin, L. Zuo, K. Gao, M. Zhang, S. B. Jo, F. Liu and A. K. Y. Jen, *Chem. Mater.*, 2019, **31**, 6770-6778.
5. C. Li, T. Xia, J. Song, H. Fu, H. S. Ryu, K. Weng, L. Ye, H. Y. Woo and Y. Sun, *J. Mater. Chem. A*, 2019, **7**, 1435-1441.
6. Z. Liang, M. Li, X. Zhang, Q. Wang, Y. Jiang, H. Tian and Y. Geng, *J. Mater. Chem. A*, 2018, **6**, 8059-8067.
7. D. Liu, B. Kan, X. Ke, N. Zheng, Z. Xie, D. Lu and Y. Liu, *Adv. Energy Mater.*, 2018, **8**, 1801618.

8. C. Li, J. Song, Y. Cai, G. Han, W. Zheng, Y. Yi, H. S. Ryu, H. Y. Woo and Y. Sun, *J. Energy Chem.*, 2020, **40**, 144-150.
9. X. Liao, X. Shi, M. Zhang, K. Gao, L. Zuo, F. Liu, Y. Chen and A. K. Jen, *Chem. Commun.*, 2019, **55**, 8258-8261.
10. W. Gao, Q. An, R. Ming, D. Xie, K. Wu, Z. Luo, Y. Zou, F. Zhang and C. Yang, *Adv. Funct. Mater.*, 2017, **27**, 1702194.
11. Y. Li, L. Zhong, F.-P. Wu, Y. Yuan, H.-J. Bin, Z.-Q. Jiang, Z. Zhang, Z.-G. Zhang, Y. Li and L.-S. Liao, *Energy Environ. Sci.*, 2016, **9**, 3429-3435.
12. D. Meng, D. Sun, C. Zhong, T. Liu, B. Fan, L. Huo, Y. Li, W. Jiang, H. Choi, T. Kim, J. Y. Kim, Y. Sun, Z. Wang and A. J. Heeger, *J. Am. Chem. Soc.*, 2016, **138**, 375-380.
13. Y. Li, D. Qian, L. Zhong, J.-D. Lin, Z.-Q. Jiang, Z.-G. Zhang, Z. Zhang, Y. Li, L.-S. Liao and F. Zhang, *Nano Energy*, 2016, **27**, 430-438.
14. Y. Yin, J. Song, F. Guo, Y. Sun, L. Zhao and Y. Zhang, *ACS Appl. Energy Mater.*, 2018, **1**, 6577-6585.
15. W. Gao, T. Liu, J. Li, Y. Xiao, G. Zhang, Y. Chen, C. Zhong, X. Lu, H. Yan and C. Yang, *J. Mater. Chem. A*, 2019, **7**, 11053-11061.
16. Y. Zhao, Z. Luo, G. Li, J. Luo, Z. G. Zhang, Y. Li and C. Yang, *Chem. Commun. (Camb)*, 2018, **54**, 9801-9804.
17. J. Zhang, W. Liu, S. Chen, S. Xu, C. Yang and X. Zhu, *J. Mater. Chem. A*, 2018, **6**, 22519-22525.
18. C. Li, J. Song, L. Ye, C. Koh, K. Weng, H. Fu, Y. Cai, Y. Xie, D. Wei, H. Y. Woo and Y. Sun, *Solar RRL*, 2019, **3**, 1800246.
19. W. Gao, Q. An, C. Zhong, Z. Luo, R. Ming, M. Zhang, Y. Zou, F. Liu, F. Zhang and C. Yang, *Chem. Sci.*, 2018, **9**, 8142-8149.
20. X. Li, C. Li, L. Ye, K. Weng, H. Fu, H. S. Ryu, D. Wei, X. Sun, H. Y. Woo and Y. Sun, *J. Mater. Chem. A*, 2019, **7**, 19348-19354.
21. L. Ye, Y. Xie, Y. Xiao, J. Song, C. Li, H. Fu, K. Weng, X. Lu, S. Tan and Y. Sun, *J. Mater. Chem. A*, 2019, **7**, 8055-8060.
22. J. Song, C. Li, L. Ye, C. Koh, Y. Cai, D. Wei, H. Y. Woo and Y. Sun, *J. Mater. Chem. A*, 2018, **6**, 18847-18852.
23. B. Gao, H. Yao, J. Hou, R. Yu, L. Hong, Y. Xu and J. Hou, *J. Mater. Chem. A*, 2018, **6**, 23644-23649.
24. W. Gao, F. Wu, T. Liu, G. Zhang, Z. Chen, C. Zhong, L. Zhu, F. Liu, H. Yan and C. Yang, *J. Mater. Chem. A*, 2019, **7**, 2412-2420.
25. W. Gao, T. Liu, C. Zhong, G. Zhang, Y. Zhang, R. Ming, L. Zhang, J. Xin, K. Wu, Y. Guo, W. Ma, H. Yan, Y. Liu and C. Yang, *ACS Energy Lett.*, 2018, **3**, 1760-1768.
26. C. Li, Y. Xie, B. Fan, G. Han, Y. Yi and Y. Sun, *J. Mater. Chem. C*, 2018, **6**, 4873-4877.
27. S. Feng, C. Zhang, Z. Bi, Y. Liu, P. Jiang, S. Ming, X. Xu, W. Ma and Z. Bo, *ACS Appl. Mater. Interfaces*, 2019, **11**, 3098-3106.
28. M. Li, Y. Zhou, J. Zhang, J. Song and Z. Bo, *J. Mater. Chem. A*, 2019, **7**, 8889-8896.
29. W. Gao, M. Zhang, T. Liu, R. Ming, Q. An, K. Wu, D. Xie, Z. Luo, C. Zhong, F. Liu, F. Zhang, H. Yan and C. Yang, *Adv. Mater.*, 2018, **30**, 1800052.
30. W. Zhai, A. Tang, B. Xiao, X. Wang, F. Chen and E. Zhou, *Sci. Bull.*, 2018, **63**, 845-852.
31. S. Feng, C. Zhang, Y. Liu, Z. Bi, Z. Zhang, X. Xu, W. Ma and Z. Bo, *Adv. Mater.*, 2017, **29**, 1703527.
32. Z. Luo, G. Li, K. Wu, Z.-G. Zhang, X. Chen, B. Qiu, L. Xue, Y. Li and C. Yang, *Org. Electron.*, 2018, **62**, 82-88.